Ultrasonics 92 (2019) 68–78

Contents lists available at ScienceDirect

Ultrasonics

journal homepage: www.elsevier.com/locate/ultras

The dispersion and attenuation of the multi-physical fields coupled waves in a piezoelectric semiconductor

Fengyu Jiao[a,b], Peijun Wei[a,b,*], Xiaoli Zhou[a,b,c], Yahong Zhou[a,b]

[a] Beijing Key Laboratory for Magneto-Photoelectrical Composite and Interface Science, University of Science and Technology Beijing, Beijing 100083, China
[b] Department of Applied Mechanics, University of Science and Technology Beijing, Beijing 100083, China
[c] School of Civil Engineering, Hebei University of Engineering, Handan 056038, China

ARTICLE INFO

Keywords:
Piezoelectric semiconductor
Coupled waves
Dispersion and attenuation
Energy flux
Reflection

ABSTRACT

The dispersion and attenuation features of the multi-physical fields coupled waves propagating in an infinite piezoelectric semiconductor and the reflection problem at a boundary which is mechanically free, electrically insulation and the dielectrically open circuit are studied in this paper. Different from the classic dielectric piezoelectric medium, there are four kinds of coupled elastic waves, i.e. the quasi-longitudinal wave (QP), the quasi-traverse wave (QSV), the electric–acoustic wave (EA) and the electron or hole carriers wave (CP), in a piezoelectric semiconductor. The influences of the steady carrier density and biasing electric field upon the dispersion and attenuation features of these coupled elastic waves and the reflection amplitude ratios are studied numerically. The energy flux of each wave and the interaction energy fluxes among all waves are also calculated, and the energy flux balance is checked. It is found that the piezoelectric semiconductor behaves like the viscoelastic solid to carry a decaying wave. The steady carrier density and biasing electric field have significant influences on the dispersion and attenuation features and can be used to regulate the propagation of the coupled elastic waves.

1. Introduction

Piezoelectric materials have been widely used to make electromechanical devices, e.g. transducer, actuator, sensor, and attracted a lot of attention in the past decades. They are usually treated as dielectric although some of them are in fact semiconductors [1]. There is no sharp division separating conductors from dielectrics. Real materials more or less have certain conductivity. Apart from the intrinsic semiconductor, a large number of semiconductors are created by the doping technology. An acoustic wave propagating in a piezoelectric crystal is always accompanied by an electric field. However, an acoustic wave propagating in a piezoelectric semiconductor is accompanied by not only an electric field but also a concentration field of charge carriers (electron and hole). The interaction of the electric field and the concentration field of charge carriers in a piezoelectric semiconductor results in the electric current. The electric current further gives rise to the acoustic dispersion and the acoustic attenuation as well as the energy transduction [2]. Weinreich et al. [3] early studied the acoustoelectric effect in a piezoelectric semiconductor of n-type, namely, the interaction between a travelling acoustic wave and mobile charge carriers. Acoustoelectric effect exists not only in the piezoelectric semiconductor but also in the composite structures of piezoelectric dielectrics and non-piezoelectric semiconductors [4–7]. In these composites, the acoustoelectric effect is due to the combination of the piezoelectric effect and semiconductor effect in the component phase. It was also found that an acoustic wave traveling in a piezoelectric semiconductor can be amplified by the biasing electric field [8–10]. This phenomenon is called acoustoelectric amplification of acoustic waves. Acoustoelectric effect and acoustoelectric amplification of acoustic waves in piezoelectric semiconductors or composites structures consisting of the piezoelectric dielectrics and non-piezoelectric semiconductors have been widely used to design acoustoelectric devices by many researchers [4,11]. Energy harvest and conversion by using piezoelectric semiconductor structures have also been studied [12–14].

For the wave propagation problems in piezoelectric semiconductors, the existing researches mainly aimed at the surface waves and the guided waves. Zhang et al. [15,16] made a theoretical study of the carrier distribution and the electromechanical fields in a free piezoelectric semiconductor rod of crystals of class 6 mm, and studied the propagation of the extensional waves in a piezoelectric semiconductor rod. Yang and Zhou [9] investigated the propagation of anti-plane (SH) wave in a piezoelectric ceramic plate carrying a thin layer of a

* Corresponding author at: Department of Applied Mechanics, University of Science and Technology Beijing, Beijing 100083, China.
E-mail address: weipj@ustb.edu.cn (P. Wei).

https://doi.org/10.1016/j.ultras.2018.09.009
Received 9 April 2018; Received in revised form 3 September 2018; Accepted 19 September 2018
Available online 20 September 2018
0041-624X/

semiconducting material on each of its major surfaces. Gu and Jin [10] studied the propagation of shear-horizontal surface waves in a piezoelectric semiconductor half-space of crystals of class 6 mm with the presence of a biasing electric field in the propagation direction. Sharma et al. [5] studied the surface waves in a piezoelectric–semiconductor composite structure. Compared with the surface waves and the guided waves in various wave guides, the study of the bulk waves in piezoelectric semiconductors is also important and interesting. Although the reflection of acoustodiffusive waves from the boundary of a classic semiconductor half-space (without consideration of the piezoelectricity) and the reflection and transmission of acoustic waves at the semiconductor/liquid interface were studied [17,18]. However, the in-depth investigation on the dispersion and attenuation features and the energy flux estimation of the multi-physical fields coupled elastic waves in the piezoelectric semiconductors are still rare.

In this paper, the dispersion and attenuation features of the multi-physical fields coupled waves in an infinite piezoelectric semiconductor are derived and the viscoelastic phenomenological analogy of the semiconductor effect (only for the dispersion and attenuation features) is first proposed. In addition, the energy flux estimation, especially, the estimation of the interaction energy flux, is provided. As a numerical example, the reflection problem at the boundary with the mechanically free, the electrically insulation and the dielectrically open circuit of a piezoelectric semiconductor half-space is considered. The amplitude ratios of various reflection waves to the incident wave are calculated and the energy flux balance is checked. The influences of the steady carrier density and biasing electric field are discussed.

2. Coupled waves in the piezoelectric semiconductor

The basic behavior of the piezoelectric semiconductor can be described by a linear phenomenological theory. We consider a p-type piezoelectric semiconductor. The constitutive equations of the piezoelectric semiconductor solid can be written as [9,10]

$$\sigma_{ij} = c_{ijkl}S_{kl} - e_{kij}E_k \tag{1a}$$

$$D_i = e_{ikl}S_{kl} + \varepsilon_{ik}E_k \tag{1b}$$

$$J_i = q\overline{p}\mu_{ij}E_j + qp\mu_{ij}\overline{E}_j - qd_{ij}p_j \tag{1c}$$

where σ_{ij} is the Cauchy stress tensor, c_{ijkl} is the elastic constant tensor, S_{kl} is the strain tensor, e_{kij} is the piezoelectric coefficient tensor, E_k is the electric field vector, D_i is the electric displacement vector, ε_{ik} is the dielectric constant tensor, J_i is the electric current vector, q is the carrier charge, $\overline{p}$ is the steady carrier density, $\overline{E}_j$ is the biasing electric field, p is the perturbation of the carrier density, μ_{ij} and d_{ij} are the carrier mobility and diffusion constants tensor, respectively. Let the z-axis be the poling direction and the material is assumed to be transversely isotropic in the oxy coordinate plane. Then, Eq. (1) reduces to

$$\begin{Bmatrix}\sigma_{xx}\\ \sigma_{yy}\\ \sigma_{zz}\\ \sigma_{yz}\\ \sigma_{zx}\\ \sigma_{xy}\end{Bmatrix} = \begin{bmatrix} c_{11} & c_{12} & c_{13} & 0 & 0 & 0 \\ c_{12} & c_{11} & c_{13} & 0 & 0 & 0 \\ c_{13} & c_{13} & c_{33} & 0 & 0 & 0 \\ 0 & 0 & 0 & c_{44} & 0 & 0 \\ 0 & 0 & 0 & 0 & c_{44} & 0 \\ 0 & 0 & 0 & 0 & 0 & 0.5(c_{11}-c_{12}) \end{bmatrix} \cdot \begin{Bmatrix} S_{xx}\\ S_{yy}\\ S_{zz}\\ 2S_{yz}\\ 2S_{zx}\\ 2S_{xy}\end{Bmatrix} - \begin{bmatrix} 0 & 0 & e_{31} \\ 0 & 0 & e_{31} \\ 0 & 0 & e_{33} \\ 0 & e_{15} & 0 \\ e_{15} & 0 & 0 \\ 0 & 0 & 0 \end{bmatrix} \cdot \begin{Bmatrix} E_x\\ E_y\\ E_z\end{Bmatrix} \tag{2a}$$

$$\begin{Bmatrix} D_x\\ D_y\\ D_z\end{Bmatrix} = \begin{bmatrix} 0 & 0 & 0 & 0 & e_{15} & 0 \\ 0 & 0 & 0 & e_{15} & 0 & 0 \\ e_{31} & e_{31} & e_{33} & 0 & 0 & 0 \end{bmatrix} \cdot \begin{Bmatrix} S_{xx}\\ S_{yy}\\ S_{zz}\\ 2S_{yz}\\ 2S_{zx}\\ 2S_{xy}\end{Bmatrix} + \begin{bmatrix} \varepsilon_{11} & 0 & 0 \\ 0 & \varepsilon_{11} & 0 \\ 0 & 0 & \varepsilon_{33} \end{bmatrix} \cdot \begin{Bmatrix} E_x\\ E_y\\ E_z\end{Bmatrix} \tag{2b}$$

$$\begin{Bmatrix} J_x\\ J_y\\ J_z\end{Bmatrix} = q\overline{p} \begin{bmatrix} \mu_{11} & 0 & 0 \\ 0 & \mu_{11} & 0 \\ 0 & 0 & \mu_{33} \end{bmatrix} \cdot \begin{Bmatrix} E_x\\ E_y\\ E_z\end{Bmatrix} + qp \begin{bmatrix} \mu_{11} & 0 & 0 \\ 0 & \mu_{11} & 0 \\ 0 & 0 & \mu_{33} \end{bmatrix} \cdot \begin{Bmatrix} \overline{E}_x\\ \overline{E}_y\\ \overline{E}_z\end{Bmatrix} - q \begin{bmatrix} d_{11} & 0 & 0 \\ 0 & d_{11} & 0 \\ 0 & 0 & d_{33} \end{bmatrix} \cdot \begin{Bmatrix} p_x\\ p_y\\ p_z\end{Bmatrix} \tag{2c}$$

where S_{ij} and E_i are defined as $S_{ij} = (u_{j,i} + u_{i,j})/2$ and $E_i = -\varphi_{,i}$, respectively. u_i is the displacement vector while φ is the electric potential. The governing equations consist of the equations of motion (Newton's law), Gauss's law of electrostatics and the conservation of charge, namely, [9,10]

$$\sigma_{ij,j} = \rho\ddot{u}_i,\ D_{i,i} = qp, \quad q\dot{p} + J_{i,i} = 0, \tag{3a,b,c}$$

where ρ is the mass density. A comma followed by an index denotes partial differentiation with respect to the coordinate associated with the index. A superimposed dot represents differentiation with respect to time. In the plane strain case, the mechanical displacement, the electric potential and the perturbation of carrier density are the functions of only x and z, namely,

$$u = \{u(x, z, t), 0, w(x, z, t)\}, \quad \varphi = \varphi(x, z, t), \quad p = p(x, z, t) \tag{4a,b,c}$$

Inserting Eq. (2) into Eq. (3) leads to

$$\begin{cases} c_{11}\frac{\partial^2 u}{\partial x^2} + c_{44}\frac{\partial^2 u}{\partial z^2} + (c_{13}+c_{44})\frac{\partial^2 w}{\partial x \partial z} + (e_{15}+e_{31})\frac{\partial^2 \varphi}{\partial x \partial z} = \rho\frac{\partial^2 u}{\partial t^2} \\ c_{44}\frac{\partial^2 w}{\partial x^2} + c_{33}\frac{\partial^2 w}{\partial z^2} + (c_{13}+c_{44})\frac{\partial^2 u}{\partial x \partial z} + e_{15}\frac{\partial^2 \varphi}{\partial x^2} + e_{33}\frac{\partial^2 \varphi}{\partial z^2} = \rho\frac{\partial^2 w}{\partial t^2} \\ e_{15}\frac{\partial^2 w}{\partial x^2} + e_{33}\frac{\partial^2 w}{\partial z^2} + (e_{15}+e_{31})\frac{\partial^2 u}{\partial x \partial z} - \varepsilon_{11}\frac{\partial^2 \varphi}{\partial x^2} - \varepsilon_{33}\frac{\partial^2 \varphi}{\partial z^2} = qp \\ \overline{p}\mu_{11}\frac{\partial^2 \varphi}{\partial x^2} + \overline{p}\mu_{33}\frac{\partial^2 \varphi}{\partial z^2} + d_{11}\frac{\partial^2 p}{\partial x^2} + d_{33}\frac{\partial^2 p}{\partial z^2} - \mu_{11}\overline{E}_x\frac{\partial p}{\partial x} - \mu_{33}\overline{E}_z\frac{\partial p}{\partial z} = \frac{\partial p}{\partial t} \end{cases} \tag{5}$$

For the wave propagation problem, the solution of Eq. (5) is of the form

$$\{u, w, \varphi, p\} = \{U_1, U_2, U_3, U_4\}\exp[i(k_x x + k_z z - \omega t)] \tag{6}$$

The wave propagating in the piezoelectric semiconductor medium will produce attenuation due to the electric current. Therefore, the wavenumber $k = k^{(r)} + ik^{(i)}$ is a complex number. The real part of k, i.e. $k^{(r)}$, indicates the wave propagation, the imaginary part of k, i.e. $k^{(i)}$, indicates the wave attenuation. When the dispersion feature of the wave is concerned, the wave is assumed to be the homogeneous wave, namely, the direction of propagation and the direction of attenuation are coincident. $k_x(=k\sin\theta)$ and $k_z(=k\cos\theta)$ are also complex values. θ is the angle that the wave propagation direction deviates from the positive z axis. ω is the angular frequency. Inserting Eq. (6) into Eq. (5) leads to

$$\begin{bmatrix} K_{11} & K_{12} & K_{13} & 0 \\ K_{21} & K_{22} & K_{23} & 0 \\ K_{31} & K_{32} & K_{33} & K_{34} \\ 0 & 0 & K_{43} & K_{44} \end{bmatrix} \cdot \begin{Bmatrix} U_1\\ U_2\\ U_3\\ U_4\end{Bmatrix} = \begin{Bmatrix} 0\\ 0\\ 0\\ 0\end{Bmatrix} \tag{7}$$

The explicit expressions of elements in the matrix **K** are given in Appendix A. The condition of existing non-trivial solution is

$$|K_{ij}(k, \theta, \omega)|_{4\times 4} = 0 \tag{8}$$

It is the dispersion equation of wave propagation. In general, for a given propagation direction θ, a curve which relates the wavenumber k

and the angular frequency ω can be obtained. The wave speed c can be calculated by $c = \omega/k^{(r)}$.

In general, Eq. (8) is a polynomial of eight orders about k, i.e. $a_8k^8 + a_7k^7 + a_6k^6 + a_5k^5 + a_4k^4 + a_3k^3 + a_2k^2 + a_1k + a_0 = 0$, The solutions of this equation stand for all possible wave modes. For the transversely isotropic piezoelectric semiconductor material, the above polynomial will reduce to $a_8k^8 + a_7k^7 + a_6k^6 + a_5k^5 + a_4k^4 + a_3k^3 + a_2k^2 = 0$. This can be derived from Appendix A. It is observed that the equation has two zeros roots which indicate that the two electric–acoustic waves (EA) reduce to the vibration modes, and the rest values of k are the complex numbers. When the biasing electric field is not considered, the polynomial will further reduce to $a_8k^8 + a_6k^6 + a_4k^4 + a_2k^2 = 0$. In this situation, the roots of the equation will be three pairs of opposite complex numbers except for zeros roots. The real part of k indicates the wavenumber while the imaginary part of k indicates the attenuation nature. These values of k imply that there are eight partial waves. Four waves of them are of the wave vector with positive projection along z axis and the other four waves with negative projection along z axis. Let k_1, k_3, k_5 and k_7 be corresponding with the quasi-longitudinal wave (QP), the quasi-traverse wave (QSV), the electric–acoustic wave (EA) (vibration mode in the infinite piezoelectric semiconductor medium) and carrier wave (CP) with the positive projection along z axis; while k_2, k_4, k_6 and k_8 are corresponding with the QP wave, QSV wave, EA wave (vibration mode in the infinite piezoelectric semiconductor medium) and CP wave with the negative projection along z axis. These partial waves are usually coupled waves with the coupled vector (U_1, U_2, U_3, U_4) which exactly reflects the coupled features among the mechanical displacement field, the electric potential field and the carrier density field. It is worth noting that the EA wave is no longer the vibration mode in the reflection problem of waves in the piezoelectric semiconductor half-space.

3. Reflection waves at the boundary

For a piezoelectric semiconductor half-space, the reflection waves from the boundary are usually inhomogeneous waves even if the incident wave is homogeneous wave. Defining θ and ϕ are the propagation angle and the attenuation angle of the incident and reflection waves, respectively, see Fig. 1. Then the generalized Snell's law can be expressed as

$$k^{\mathrm{I}(r)}\sin\theta^{\mathrm{I}} = k_{\mathrm{QP}}^{\mathrm{R}(r)}\sin\theta_{\mathrm{QP}}^{\mathrm{R}} = k_{\mathrm{QSV}}^{\mathrm{R}(r)}\sin\theta_{\mathrm{QSV}}^{\mathrm{R}} = k_{\mathrm{EA}}^{\mathrm{R}(r)}\sin\theta_{\mathrm{EA}}^{\mathrm{R}} = k_{\mathrm{CP}}^{\mathrm{R}(r)}\sin\theta_{\mathrm{CP}}^{\mathrm{R}} = k_x^{(r)} \tag{9}$$

$$k^{\mathrm{I}(i)}\sin\phi^{\mathrm{I}} = k_{\mathrm{QP}}^{\mathrm{R}(i)}\sin\phi_{\mathrm{QP}}^{\mathrm{R}} = k_{\mathrm{QSV}}^{\mathrm{R}(i)}\sin\phi_{\mathrm{QSV}}^{\mathrm{R}} = k_{\mathrm{EA}}^{\mathrm{R}(i)}\sin\phi_{\mathrm{EA}}^{\mathrm{R}} = k_{\mathrm{CP}}^{\mathrm{R}(i)}\sin\phi_{\mathrm{CP}}^{\mathrm{R}} = k_x^{(i)} \tag{10}$$

where the superscript "I" and "R" indicate the quantities related with the incident wave and the reflection waves, respectively. The incident wave is considered as the homogeneous wave in the present work, therefore, $\theta^{\mathrm{I}} = \phi^{\mathrm{I}}$ in Eqs. (9) and (10). The propagation direction and attenuation direction of the reflection waves can be determined by

$$\theta_q^{\mathrm{R}} = \arcsin\left(\frac{k^{\mathrm{I}(r)}}{k_q^{\mathrm{R}(r)}}\sin\theta^{\mathrm{I}}\right), \quad q = \mathrm{QP,QSV,EA,CP} \tag{11}$$

$$\phi_q^{\mathrm{R}} = \arcsin\left(\frac{k^{\mathrm{I}(i)}}{k_q^{\mathrm{R}(i)}}\sin\theta^{\mathrm{I}}\right), \quad q = \mathrm{QP,QSV,EA,CP} \tag{12}$$

Define the amplitude ratios of each coupled wave ($q = 1, 2, \cdots, 8$)

$$\begin{cases} G_q = \dfrac{U_{2q}}{U_{1q}} = \dfrac{K_{21}(k_{zq})\cdot K_{13}(k_{zq}) - K_{11}(k_{zq})\cdot K_{23}(k_{zq})}{K_{12}(k_{zq})\cdot K_{23}(k_{zq}) - K_{13}(k_{zq})\cdot K_{22}(k_{zq})} \\ H_q = \dfrac{U_{3q}}{U_{1q}} = \dfrac{K_{11}(k_{zq})\cdot K_{22}(k_{zq}) - K_{12}(k_{zq})\cdot K_{21}(k_{zq})}{K_{12}(k_{zq})\cdot K_{23}(k_{zq}) - K_{13}(k_{zq})\cdot K_{22}(k_{zq})} \\ Q_q = \dfrac{U_{4q}}{U_{1q}} = -\dfrac{K_{43}(k_{zq})}{K_{44}(k_{zq})}H_q \end{cases} \tag{13}$$

Then, the displacement, the electric potential, the perturbation of carrier density, the stress, the electric displacement and the electric current created by the incident wave and the reflection waves can be expressed as

$$\{u, w, \varphi, p\} = \sum_{q=1}^{8}\{1, G_q, H_q, Q_q\}U_{1q}\exp[i(k_x x + k_{zq}z - \omega t)] \tag{14}$$

$$\{\sigma_{zx}, \sigma_{zz}, \sigma_{xx}\} = \sum_{q=1}^{8} i\{F_{1q}, F_{2q}, F_{3q}\}U_{1q}\exp[i(k_x x + k_{zq}z - \omega t)] \tag{15}$$

$$\{D_z, D_x\} = \sum_{q=1}^{8} i\{F_{4q}, F_{5q}\}U_{1q}\exp[i(k_x x + k_{zq}z - \omega t)] \tag{16}$$

$$\{J_z, J_x\} = \sum_{q=1}^{8}\{F_{6q}, F_{7q}\}U_{1q}\exp[i(k_x x + k_{zq}z - \omega t)] \tag{17}$$

The explicit expressions of $F_{iq}(i = 1-7)$ are given in Appendix B.

For the mechanically traction-free, electrically insulation and the dielectrically open circuit boundary, the boundary conditions can be expressed as

$$\sigma_{zx} = 0, \quad \sigma_{zz} = 0, \quad D_z = 0, \quad J_z = 0, \quad \text{at } z = 0 \tag{18}$$

These boundary conditions lead to

$$\begin{bmatrix} F_{11} & F_{13} & F_{15} & F_{17} \\ F_{21} & F_{23} & F_{25} & F_{27} \\ F_{41} & F_{43} & F_{45} & F_{47} \\ F_{61} & F_{63} & F_{65} & F_{67} \end{bmatrix}\begin{Bmatrix} L_1 \\ L_2 \\ L_3 \\ L_4 \end{Bmatrix} = -\begin{Bmatrix} F_{1q} \\ F_{2q} \\ F_{4q} \\ F_{6q} \end{Bmatrix} \tag{19}$$

where $L_1 = U_{11}/U_{1q}$, $L_2 = U_{13}/U_{1q}$, $L_3 = U_{15}/U_{1q}$, $L_4 = U_{17}/U_{1q}$ are the amplitude ratios of various reflection waves to the incident wave. The subscript q indicates the type of the incident wave with $q = 2$ for the incident QP wave while $q = 4$ for the incident QSV wave.

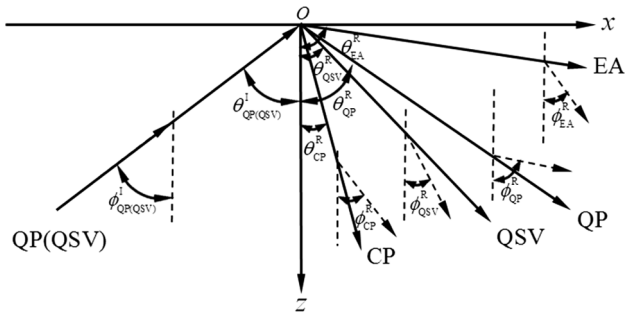

Fig. 1. The propagation angle θ and the attenuation angle ϕ of the incidence and reflection waves at the boundary.

4. Energy flux balance

Different from the classical elastic solid, the interaction energy fluxes play an important role in the viscoelastic medium [19] when the energy flux balance at an interface is concerned. Because the viscoelastic effect and the semiconductor effect are similar on the propagation behavior of waves in the infinite and semi-infinite medium, the interaction energy fluxes in the piezoelectric semiconductor medium should not be neglected when considering the energy flux balance at the boundary.

In the piezoelectric medium, the energy flux can be evaluated by [20–23]

$$P_i(t) = -\sigma_{ij}\dot{u}_j + \varphi\dot{D}_i \tag{20}$$

when the semiconductor effects are taken into considered, Eq. (20) should be modified as

$$P_i(t) = -\sigma_{ij}\dot{u}_j + \varphi(\dot{D}_i + J_i) \tag{21}$$

The first term presents the contribution of mechanical field. The second term presents the contribution of the poling charge while the third term presents the contribution of space charge or charge carriers in the piezoelectric semiconductor medium. The mean energy flux, namely, the time-average Umov-Poynting vector **P** in a period is

$$\mathbf{P} = -\frac{1}{2}\mathrm{Re}[(\sigma_{xx}\dot{u}^* + \sigma_{xz}\dot{w}^* - \varphi\dot{D}_x^* - \varphi J_x^*)\mathbf{e}_x + (\sigma_{zx}\dot{u}^* + \sigma_{zz}\dot{w}^* - \varphi\dot{D}_z^* - \varphi J_z^*)\mathbf{e}_z] \tag{22}$$

where the superscript "∗" indicates the conjugated complex. $\mathbf{e}_x$ and $\mathbf{e}_z$ are the unit vectors of coordinate axes. For the boundary conditions, i.e. Eq. (18), the normal component of the time-average Umov-Poynting vector **P** should be zero, namely,

$$-\frac{1}{2}\mathrm{Re}(\sigma_{zx}\dot{u}^* + \sigma_{zz}\dot{w}^* - \varphi\dot{D}_z^* - \varphi J_z^*) = 0 \tag{23}$$

where

$$u = u_{QP(QSV)^I} + u_{QP^R} + u_{QSV^R} + u_{EA^R} + u_{CP^R} \tag{24}$$

$$\sigma_{zz} = \sigma_{zz(QP(QSV)^I)} + \sigma_{zz(QP^R)} + \sigma_{zz(QSV^R)} + \sigma_{zz(EA^R)} + \sigma_{zz(CP^R)} \tag{25}$$

The other quantities can be understood similarly. Denoting the normal component of the energy flux by Q, Eq. (23) leads to

$$\begin{aligned} &Q_{QP(QSV)^I} + Q_{QP^R} + Q_{QSV^R} + Q_{EA^R} + Q_{CP^R} + Q_{QP(QSV)^IQP^R} \\ &+ Q_{QP(QSV)^IQSV^R} + Q_{QP(QSV)^IEA^R} \\ &+ Q_{QP(QSV)^ICP^R} + Q_{QP^RQSV^R} + Q_{QP^REA^R} + Q_{QP^RCP^R} + Q_{QSV^REA^R} + Q_{QSV^RCP^R} \\ &+ Q_{EA^RCP^R} = 0 \end{aligned} \tag{26}$$

where

$$\begin{aligned} -2Q_{QP(QSV)^I} = \mathrm{Re}[&\sigma_{zx(QP(QSV)^I)}\dot{u}^*_{QP(QSV)^I} + \sigma_{zz(QP(QSV)^I)}\dot{w}^*_{QP(QSV)^I} \\ &-\varphi_{QP(QSV)^I}(\dot{D}^*_{z(QP(QSV)^I)} + J^*_{z(QP(QSV)^I)})] \end{aligned} \tag{27a}$$

$$-2Q_{QP^R} = \mathrm{Re}[\sigma_{zx(QP^R)}\dot{u}^*_{QP^R} + \sigma_{zz(QP^R)}\dot{w}^*_{QP^R} - \varphi_{QP^R}(\dot{D}^*_{z(QP^R)} + J^*_{z(QP^R)})] \tag{27b}$$

$$\begin{aligned} -2Q_{QSV^R} = \mathrm{Re}[&\sigma_{zx(QSV^R)}\dot{u}^*_{QSV^R} + \sigma_{zz(QSV^R)}\dot{w}^*_{QSV^R} \\ &-\varphi_{QSV^R}(\dot{D}^*_{z(QSV^R)} + J^*_{z(QSV^R)})] \end{aligned} \tag{27c}$$

$$-2Q_{EA^R} = \mathrm{Re}[\sigma_{zx(EA^R)}\dot{u}^*_{EA^R} + \sigma_{zz(EA^R)}\dot{w}^*_{EA^R} - \varphi_{EA^R}(\dot{D}^*_{z(EA^R)} + J^*_{z(EA^R)})] \tag{27d}$$

$$-2Q_{CP^R} = \mathrm{Re}[\sigma_{zx(CP^R)}\dot{u}^*_{CP^R} + \sigma_{zz(CP^R)}\dot{w}^*_{CP^R} - \varphi_{CP^R}(\dot{D}^*_{z(CP^R)} + J^*_{z(CP^R)})] \tag{27e}$$

$$\begin{aligned} -2Q_{QP(QSV)^IQP^R} = \mathrm{Re}[&\sigma_{zx(QP(QSV)^I)}\dot{u}^*_{QP^R} + \sigma_{zx(QP^R)}\dot{u}^*_{QP(QSV)^I} \\ &+ \sigma_{zz(QP(QSV)^I)}\dot{w}^*_{QP^R} + \sigma_{zz(QP^R)}\dot{w}^*_{QP(QSV)^I} \\ &- \varphi_{QP(QSV)^I}(\dot{D}^*_{z(QP^R)} + J^*_{z(QP^R)}) - \varphi_{QP^R}(\dot{D}^*_{z(QP(QSV)^I)} + J^*_{z(QP(QSV)^I)})] \end{aligned} \tag{27f}$$

$$\begin{aligned} -2Q_{QP(QSV)^IQSV^R} = \mathrm{Re}[&\sigma_{zx(QP(QSV)^I)}\dot{u}^*_{QSV^R} + \sigma_{zx(QSV^R)}\dot{u}^*_{QP(QSV)^I} \\ &+ \sigma_{zz(QP(QSV)^I)}\dot{w}^*_{QSV^R} + \sigma_{zz(QSV^R)}\dot{w}^*_{QP(QSV)^I} \\ &- \varphi_{QP(QSV)^I}(\dot{D}^*_{z(QSV^R)} + J^*_{z(QSV^R)}) - \varphi_{QSV^R}(\dot{D}^*_{z(QP(QSV)^I)} + J^*_{z(QP(QSV)^I)})] \end{aligned} \tag{27g}$$

$$\begin{aligned} -2Q_{QP(QSV)^IEA^R} = \mathrm{Re}[&\sigma_{zx(QP(QSV)^I)}\dot{u}^*_{EA^R} + \sigma_{zx(EA^R)}\dot{u}^*_{QP(QSV)^I} \\ &+ \sigma_{zz(QP(QSV)^I)}\dot{w}^*_{EA^R} + \sigma_{zz(EA^R)}\dot{w}^*_{QP(QSV)^I} \\ &- \varphi_{QP(QSV)^I}(\dot{D}^*_{z(EA^R)} + J^*_{z(EA^R)}) - \varphi_{EA^R}(\dot{D}^*_{z(QP(QSV)^I)} + J^*_{z(QP(QSV)^I)})] \end{aligned} \tag{27h}$$

$$\begin{aligned} -2Q_{QP(QSV)^ICP^R} = \mathrm{Re}[&\sigma_{zx(QP(QSV)^I)}\dot{u}^*_{CP^R} + \sigma_{zx(CP^R)}\dot{u}^*_{QP(QSV)^I} \\ &+ \sigma_{zz(QP(QSV)^I)}\dot{w}^*_{CP^R} + \sigma_{zz(CP^R)}\dot{w}^*_{QP(QSV)^I} \\ &- \varphi_{QP(QSV)^I}(\dot{D}^*_{z(CP^R)} + J^*_{z(CP^R)}) - \varphi_{CP^R}(\dot{D}^*_{z(QP(QSV)^I)} + J^*_{z(QP(QSV)^I)})] \end{aligned} \tag{27i}$$

$$\begin{aligned} -2Q_{QP^RQSV^R} = \mathrm{Re}[&\sigma_{zx(QP^R)}\dot{u}^*_{QSV^R} + \sigma_{zx(QSV^R)}\dot{u}^*_{QP^R} + \sigma_{zz(QP^R)}\dot{w}^*_{QSV^R} \\ &+ \sigma_{zz(QSV^R)}\dot{w}^*_{QP^R} \\ &- \varphi_{QP^R}(\dot{D}^*_{z(QSV^R)} + J^*_{z(QSV^R)}) - \varphi_{QSV^R}(\dot{D}^*_{z(QP^R)} + J^*_{z(QP^R)})] \end{aligned} \tag{27j}$$

$$\begin{aligned} -2Q_{QP^REA^R} = \mathrm{Re}[&\sigma_{zx(QP^R)}\dot{u}^*_{EA^R} + \sigma_{zx(EA^R)}\dot{u}^*_{QP^R} + \sigma_{zz(QP^R)}\dot{w}^*_{EA^R} \\ &+ \sigma_{zz(EA^R)}\dot{w}^*_{QP^R} \\ &- \varphi_{QP^R}(\dot{D}^*_{z(EA^R)} + J^*_{z(EA^R)}) - \varphi_{EA^R}(\dot{D}^*_{z(QP^R)} + J^*_{z(QP^R)})] \end{aligned} \tag{27k}$$

$$\begin{aligned} -2Q_{QP^RCP^R} = \mathrm{Re}[&\sigma_{zx(QP^R)}\dot{u}^*_{CP^R} + \sigma_{zx(CP^R)}\dot{u}^*_{QP^R} + \sigma_{zz(QP^R)}\dot{w}^*_{CP^R} \\ &+ \sigma_{zz(CP^R)}\dot{w}^*_{QP^R} \\ &- \varphi_{QP^R}(\dot{D}^*_{z(CP^R)} + J^*_{z(CP^R)}) - \varphi_{CP^R}(\dot{D}^*_{z(QP^R)} + J^*_{z(QP^R)})] \end{aligned} \tag{27l}$$

$$\begin{aligned} -2Q_{QSV^REA^R} = \mathrm{Re}[&\sigma_{zx(QSV^R)}\dot{u}^*_{EA^R} + \sigma_{zx(EA^R)}\dot{u}^*_{QSV^R} + \sigma_{zz(QSV^R)}\dot{w}^*_{EA^R} \\ &+ \sigma_{zz(EA^R)}\dot{w}^*_{QSV^R} \\ &- \varphi_{QSV^R}(\dot{D}^*_{z(EA^R)} + J^*_{z(EA^R)}) - \varphi_{EA^R}(\dot{D}^*_{z(QSV^R)} + J^*_{z(QSV^R)})] \end{aligned} \tag{27m}$$

$$\begin{aligned} -2Q_{QSV^RCP^R} = \mathrm{Re}[&\sigma_{zx(QSV^R)}\dot{u}^*_{CP^R} + \sigma_{zx(CP^R)}\dot{u}^*_{QSV^R} + \sigma_{zz(QSV^R)}\dot{w}^*_{CP^R} \\ &+ \sigma_{zz(CP^R)}\dot{w}^*_{QSV^R} \\ &- \varphi_{QSV^R}(\dot{D}^*_{z(CP^R)} + J^*_{z(CP^R)}) - \varphi_{CP^R}(\dot{D}^*_{z(QSV^R)} + J^*_{z(QSV^R)})] \end{aligned} \tag{27n}$$

$$\begin{aligned} -2Q_{EA^RCP^R} = \mathrm{Re}[&\sigma_{zx(EA^R)}\dot{u}^*_{CP^R} + \sigma_{zx(CP^R)}\dot{u}^*_{EA^R} + \sigma_{zz(EA^R)}\dot{w}^*_{CP^R} \\ &+ \sigma_{zz(CP^R)}\dot{w}^*_{EA^R} \\ &- \varphi_{EA^R}(\dot{D}^*_{z(CP^R)} + J^*_{z(CP^R)}) - \varphi_{CP^R}(\dot{D}^*_{z(EA^R)} + J^*_{z(EA^R)})] \end{aligned} \tag{27o}$$

in Eq. (27), Q_{QP^R} indicates the energy flux of the reflection QP, and $Q_{QP^RQSV^R}$ indicates the interaction energy flux between the reflection QP wave and reflection QSV wave. The rest can be understood similarly. In the classical elastic situation, these interaction energy fluxes vanish. The explicit expressions of Eq. (27)are given in Appendix C.

The energy reflection coefficients are defined as

$$E_{QP^R} = \frac{Q_{QP^R}}{Q_{QP(QSV)^I}}, \quad E_{QSV^R} = \frac{Q_{QSV^R}}{Q_{QP(QSV)^I}}, \quad E_{EA^R} = \frac{Q_{EA^R}}{Q_{QP(QSV)^I}}, \quad E_{CP^R} = \frac{Q_{CP^R}}{Q_{QP(QSV)^I}}$$

Similarly, $I_{QP(QSV)^IQP^R}$, $I_{QP(QSV)^IQSV^R}$, $I_{QP(QSV)^IEA^R}$, $I_{QP(QSV)^ICP^R}$, $I_{QP^RQSV^R}$, $I_{QP^REA^R}$, $I_{QP^RCP^R}$, $I_{QSV^REA^R}$, $I_{QSV^RCP^R}$ and $I_{EA^RCP^R}$ represent the ratios of $Q_{QP(QSV)^IQP^R}$, $Q_{QP(QSV)^IQSV^R}$, $Q_{QP(QSV)^IEA^R}$, $Q_{QP(QSV)^ICP^R}$, $Q_{QP^RQSV^R}$, $Q_{QP^REA^R}$, $Q_{QP^RCP^R}$, $Q_{QSV^REA^R}$, $Q_{QSV^RCP^R}$ and $Q_{EA^RCP^R}$ with respect to $Q_{QP(QSV)^I}$, respectively. Then, the energy flux balance equation Eq. (26) can be rewritten as

$$\begin{aligned} E = &-E_{QP^R} - E_{QSV^R} - E_{EA^R} - E_{CP^R} - I_{QP(QSV)^IQP^R} - I_{QP(QSV)^IQSV^R} - I_{QP(QSV)^IEA^R} \\ &- I_{QP(QSV)^IEA^R} - I_{QP^RQSV^R} - I_{QP^REA^R} - I_{QP^RCP^R} - I_{QSV^REA^R} - I_{QSV^RCP^R} - I_{EA^RCP^R} = 1 \end{aligned} \tag{28}$$

Eq. (28) can be used to validate the numerical results in the next section.

5. The numerical results and discussion

It is known that the dispersion curves, attenuation coefficients and reflection coefficients $L_i\,(i = 1–4)$ are all dependent upon the material constants of the piezoelectric semiconductor solid, the steady carrier

Table 1
The physical constants of ZnO [21,24,25].

Material	C_{11}	C_{33}	C_{13}	C_{44}	e_{31}	e_{33}	e_{15}	ρ
ZnO	209.7	210.9	105.1	42.47	−0.573	1.32	−0.48	5680
Material	d_{11}	d_{33}	μ_{11}	μ_{33}	ε_{11}	ε_{33}	q	
ZnO	0.0208	0.0208	0.8	0.8	7.57	9.031	1.602	

C_{ij} in GPa, e_{ij} in C/m^2, ρ in kg/m^3, d_{ij} in cm^2/s, μ_{ij} in cm^2/Vs, ε_{ij} in 10^{-11} C/Vm, q in 10^{-19} C.

density, the biasing electric field, the angular frequency ω and the incident angle θ of the incident wave. In the present numerical example, the main concerns focus on the effects of the steady carrier density and biasing electric field. For convenience, the non-dimensional forms of the biasing electric field are introduced, namely, $\gamma_x = \mu_{11}\overline{E}_x\sqrt{\rho/c_{44}}$, $\gamma_z = \mu_{11}\overline{E}_z\sqrt{\rho/c_{44}}$, and $\gamma = \gamma_x\mathbf{e}_x + \gamma_z\mathbf{e}_z$. The piezoelectric semiconductor solid ZnO is considered in the present work. The material constants of ZnO are listed in Table 1. According to the literatures [24,25], the mobilities of holes are between 0.5 cm^2/Vs and 1 cm^2/Vs, the steady carrier densities are between 2×10^{17} cm^{-3} and 10^{18} cm^{-3} in the nitrogen-doped p-type ZnO piezoelectric semiconductor material. The value of mobility of holes is regarded as 0.8 cm^2/Vs in this paper, and the steady carrier density is discussed in the range of 2×10^{17} - 10^{18} cm^{-3}. $d_{11} = \mu_{11}kT/q$ is used [10], k is the Boltzmann constant and T is the absolute temperature. At room temperature, $kT/q = 0.026$ V [10], The assumption, i.e. $\mu_{33} = \mu_{11}$ and $d_{33} = d_{11}$, adopted in the literature [26], is retained.

Figs. 2 and 3 show the phase velocities of QP and QSV waves propagating in the piezoelectric semiconductor medium. $\overline{C}_{QP}$ is the phase velocity ratio of QP waves propagating in the piezoelectric semiconductor solid and in the classical piezoelectric dielectric solid (without electric current) with the same propagation direction. $\overline{C}_{QSV}$ can be understood similarly. but $\overline{C}_{CP}$ is the phase velocity ratio of CP wave propagating in the piezoelectric semiconductor solid and QP wave propagating in the classical piezoelectric dielectric solid (without electric current) with the same propagation direction. It is observed that the dispersion feature of the coupled waves in the piezoelectric semiconductor medium is very similar with the dispersion feature in the standard linear viscoelastic solid [27–29]. The phase velocities of QP and QSV waves at the higher frequency and the lower frequency are both nearly independent of the angular frequency. There is a frequency zone only in which the phase velocities are sensitive to the angular frequency. This zone is hereafter called the frequency sensitive zone. Because the complex modulus of the standard linear viscoelastic solid has also a frequency sensitive zone and nearly independent of the angular frequency out of the zone, the piezoelectric semiconductor solid is similar to the standard linear viscoelastic solid with respect of the dispersion and the attenuation. The phase velocities of QP and QSV waves propagating in the piezoelectric semiconductor solid are smaller than that in the piezoelectric dielectric solid at the lower frequency within the frequency sensitive zone and gradually approach to that in the piezoelectric dielectric solid at the higher frequency. The steady carrier density and the biasing electric field have both evident influences on the dispersion features. The frequency sensitive zone shifts toward the high frequency with the increasing of the steady carrier density while toward the high frequency first, then, gradually shifts toward the low frequency with the increasing of the biasing electric field. The phase velocity of the carrier wave, i.e. $\overline{C}_{CP}$, gradually increases with the increasing of the angular frequency and is only sensitive to the steady carrier density and the biasing electric field at the lower frequency. EA wave reduces to the vibration mode in the infinite piezoelectric semiconductor solid. Therefore, no dispersion curves are provided for EA wave in Figs. 2 and 3.

Figs. 4 and 5 show the attenuation features of QP wave, QSV wave and CP wave propagating in the piezoelectric semiconductor medium. There is also a frequency sensitive zone for the attenuation features of QP wave and QSV wave. The increasing of the steady carrier density makes the attenuation coefficients of QP wave and QSV wave increasing evidently within this zone. CP wave is only sensitive to the steady carrier density at the lower frequency. Different from the steady carrier density, the biasing electric field along the propagation direction has much complicated influences on the attenuation features. Fig. 5a shows the attenuation coefficients of the QP and QSV waves are the positive value when the biasing electric field is smaller while the attenuation coefficients become the negative value when the biasing electric field exceeds a threshold value. It implies that QP and QSV waves become the amplification waves from the attenuation waves with the increasing of the biasing electric field. This phenomenon is called “acoustoelectric amplification effects” [9,10] and can be used to manipulate the wave propagation. But the threshold value corresponding to the QP wave is larger than the threshold value corresponding to the QSV wave. It can be explained by that the phase velocity of QP wave is larger than the phase velocity of QSV wave in the same propagation direction and the amplification wave appears when the drift speed of the charge carrier under the biasing electric field exceeds the phase velocity of QP wave or QSV wave [9,10]. Fig. 5b shows the attenuation coefficient of the CP wave gradually decreases with the increasing of the biasing electric field, but it is always a positive value, this implies that the CP wave is always an attenuation wave.

Fig. 6 shows the influences of the steady carrier density on the reflection amplitude ratios in the case of incident QP wave. It is observed that the reflection QP wave and QSV wave are not sensitive to the steady carrier density while EA wave and CP wave are very sensitive to the steady carrier density. The reflection amplitude ratios of the EA wave and CP wave decrease monotonously with the increasing of the steady carrier density. The influences of the steady carrier density on the reflection angles and the attenuation angles are shown in Figs. 7 and 8. The reflection angles and attenuation angles of the QP wave and QSV wave are not sensitive to the steady carrier density and thus are not provided here. It is observed that the reflection angles of the EA wave

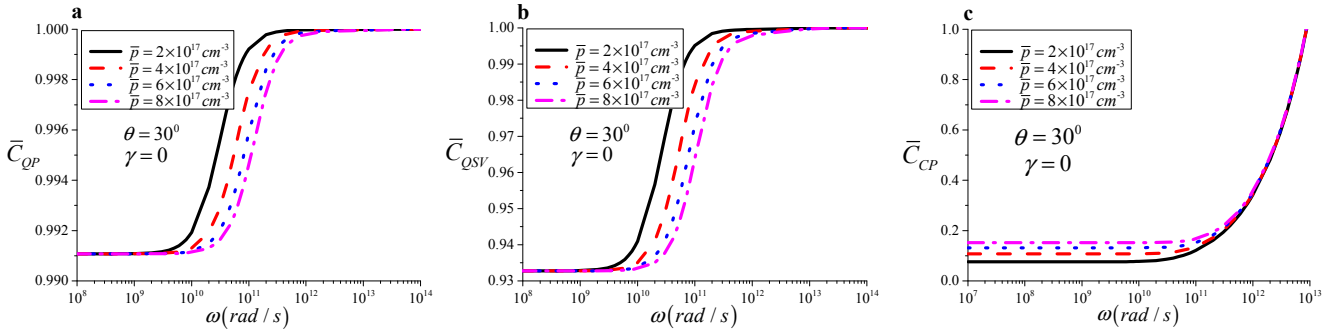

Fig. 2. The influences of the steady carrier density on the dispersion curves.

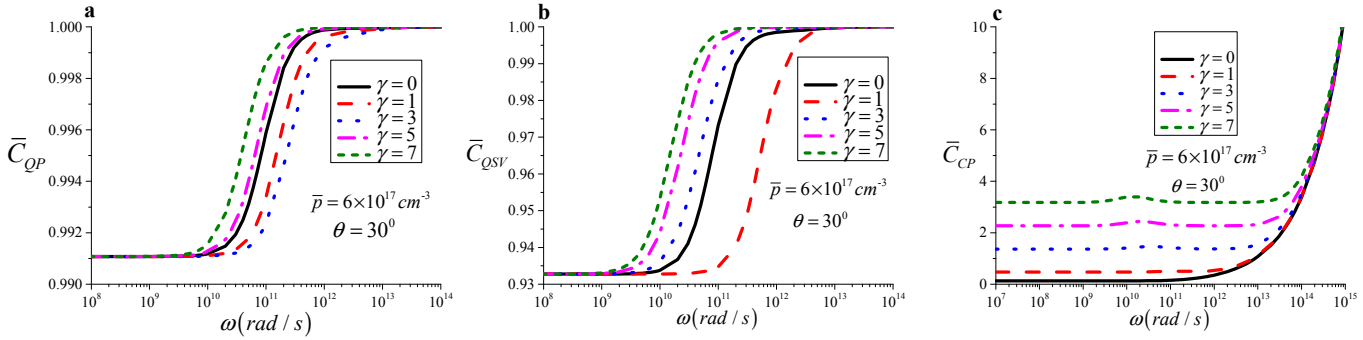

Fig. 3. The influences of the biasing electric field on the dispersion curves.

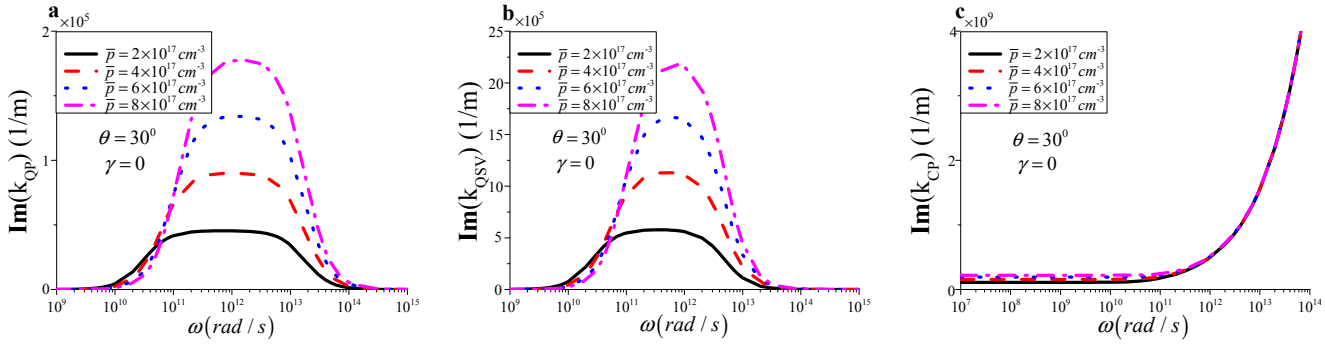

Fig. 4. The influences of the steady carrier density on the attenuation coefficients.

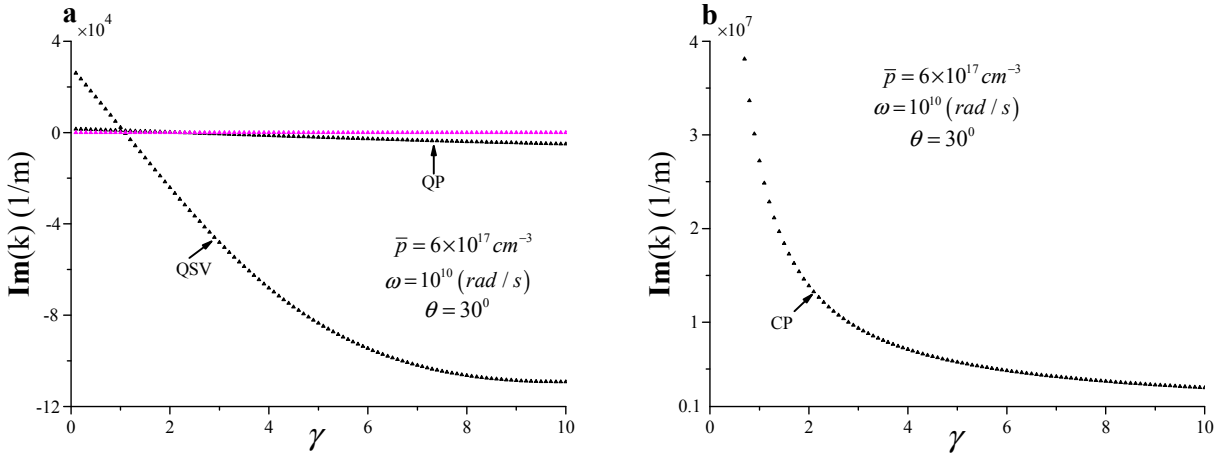

Fig. 5. The attenuation coefficients of the waves vary with the biasing electric field.

and CP wave increase when the steady carrier density increases. The reflection angle of the EA wave gradually increases first and reaches 90° at about 70° of the incident angle, then gradually decreases with the increasing of the incident angle. This implies that the reflection EA wave is a bulk wave, in general, although its propagation direction is near the surface. In contrast, EA wave is always a surface wave in the classical piezoelectric half-space. Fig. 8 shows the attenuation angles of the reflection EA wave and CP wave. It is found that the attenuation angles are usually small. This implies that the attenuation directions of the reflection EA wave and CP wave are near the normal direction of the boundary. When the incident angle is about 42°, the attenuation directions of the reflection EA wave and CP wave become the exact normal direction of the boundary.

Next, let us investigate the influences of the biasing electric field. Fig. 9 shows the influences of the biasing electric field on the reflection amplitude ratios in the case of incident QP wave. It is observed that the reflection amplitude ratios of the QP wave, QSV wave and CP wave are not sensitive to the biasing electric field while EA wave is very sensitive to the biasing electric field. The reflection amplitude ratio of EA wave decreases first then increases when the biasing electric field gradually increases. The variations of the reflection angles of the EA wave and CP wave with the biasing electric field are shown in Fig. 10. The variations of the reflection angles with the incident angle are not monotonous. There is a peak for the CP wave while there are two peaks for the EA wave. When the biasing electric field increases, the incident angles corresponding with these peaks gradually become small. The influences of the biasing electric field on the attenuation angles of the reflection EA wave and CP wave are shown in Fig. 11. It is observed that the attenuation angles are near zero. This implies that the attenuation directions of the reflection EA wave and CP wave are almost the normal direction of the boundary. When the incident angle is about 42°, the attenuation directions are exactly the normal direction of the boundary.

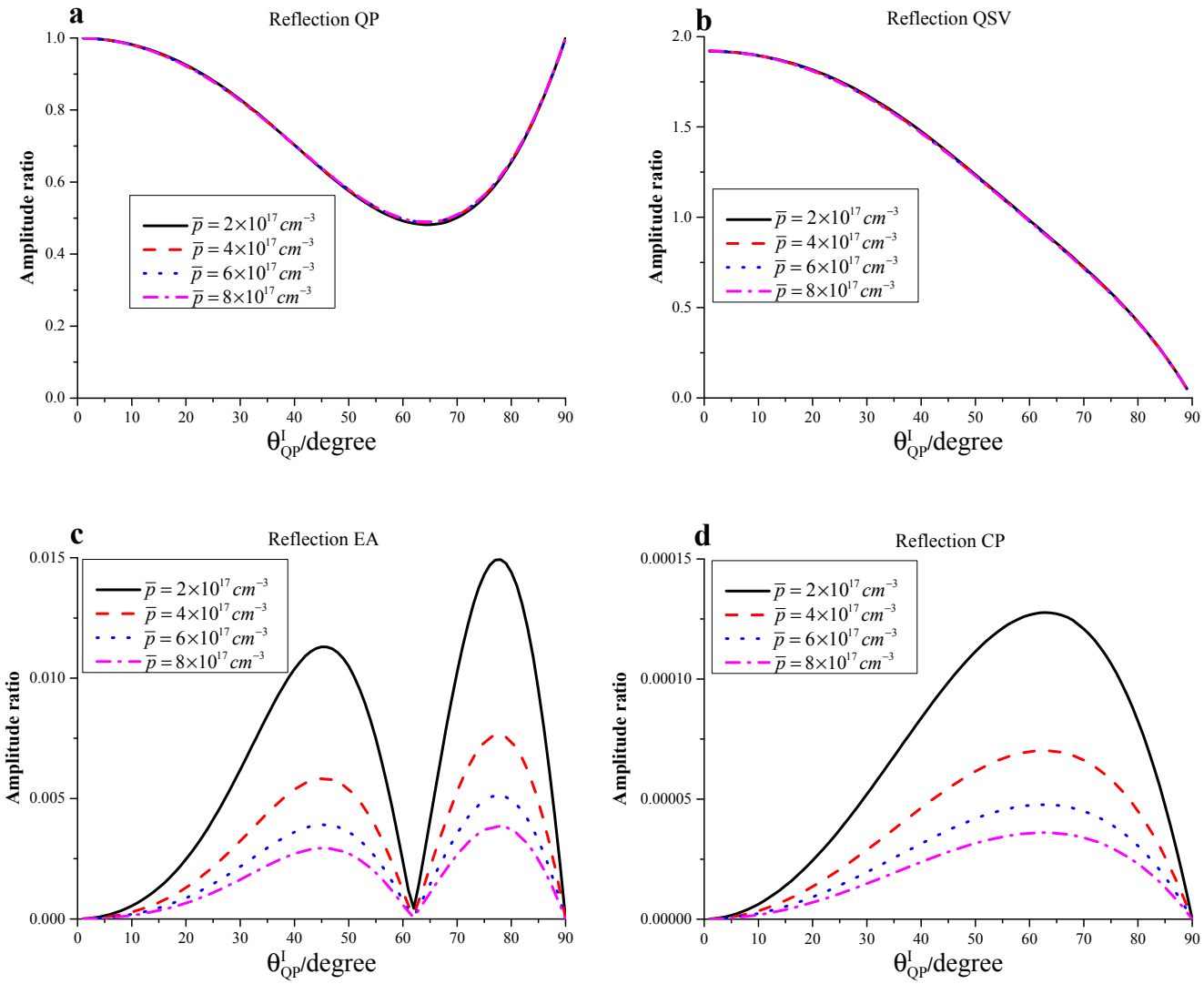

Fig. 6. The influences of the steady carrier density on the reflection amplitude ratios in the case of incident QP wave ($\gamma = 0$, $\omega = 10^{10}$ rad/s).

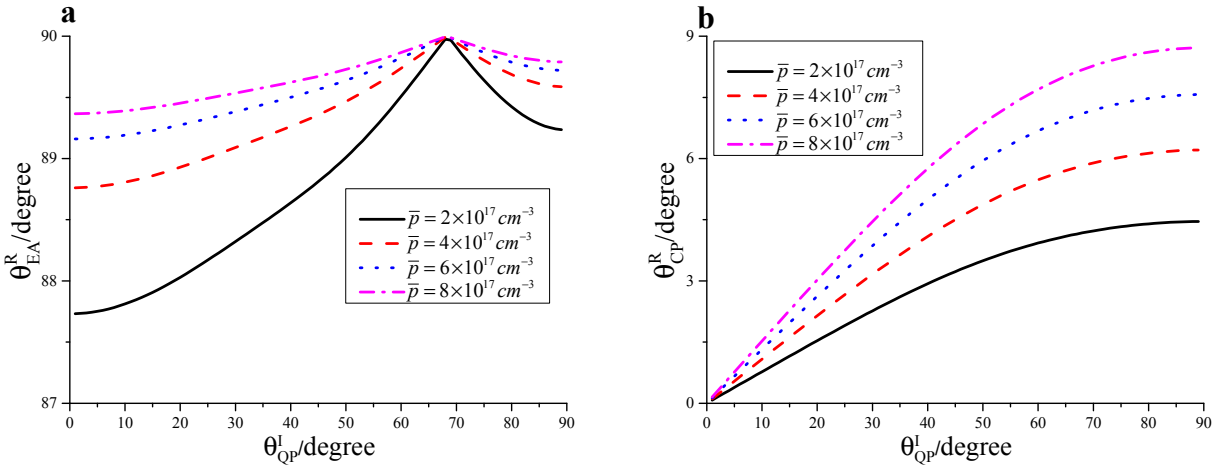

Fig. 7. The influences of the steady carrier density on the reflection angles in the case of incident QP wave ($\gamma = 0$, $\omega = 10^{10}$ rad/s).

The particular incident angle can be called the normal attenuation incident angle. It is observed that the existence of the biasing electric field creates the new normal attenuation incident angles. The influences of the biasing electric field on the reflection and attenuation angles of the QP wave and QSV wave are not sensitive and thus the corresponding figures are not provided.

In order to validate the numerical results obtained, the energy flux balance check is performed. Due to the attenuation nature of the multi-

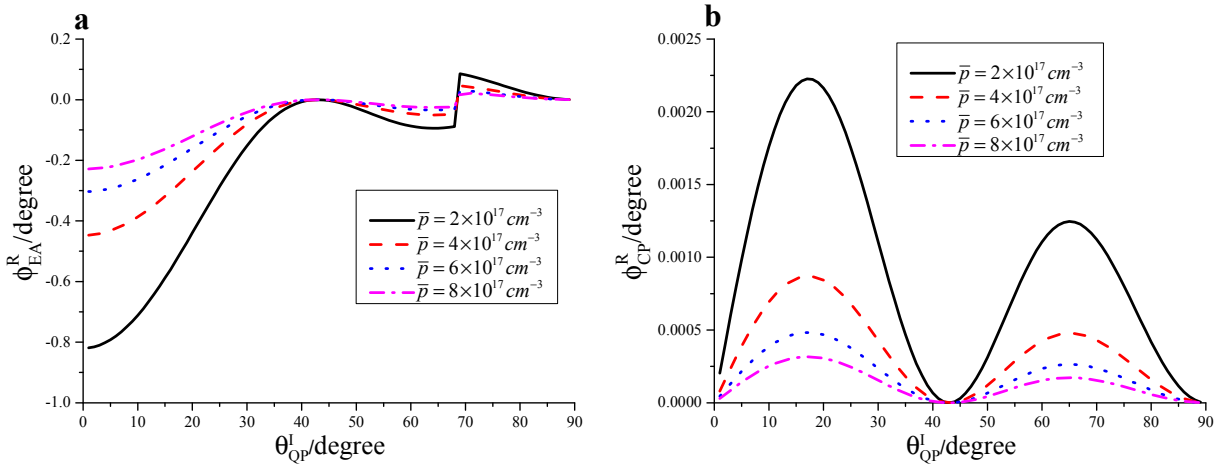

Fig. 8. The influences of the steady carrier density on the attenuation angles of the reflection waves in the case of incident QP wave ($\gamma = 0$, $\omega = 10^{10}$ rad/s).

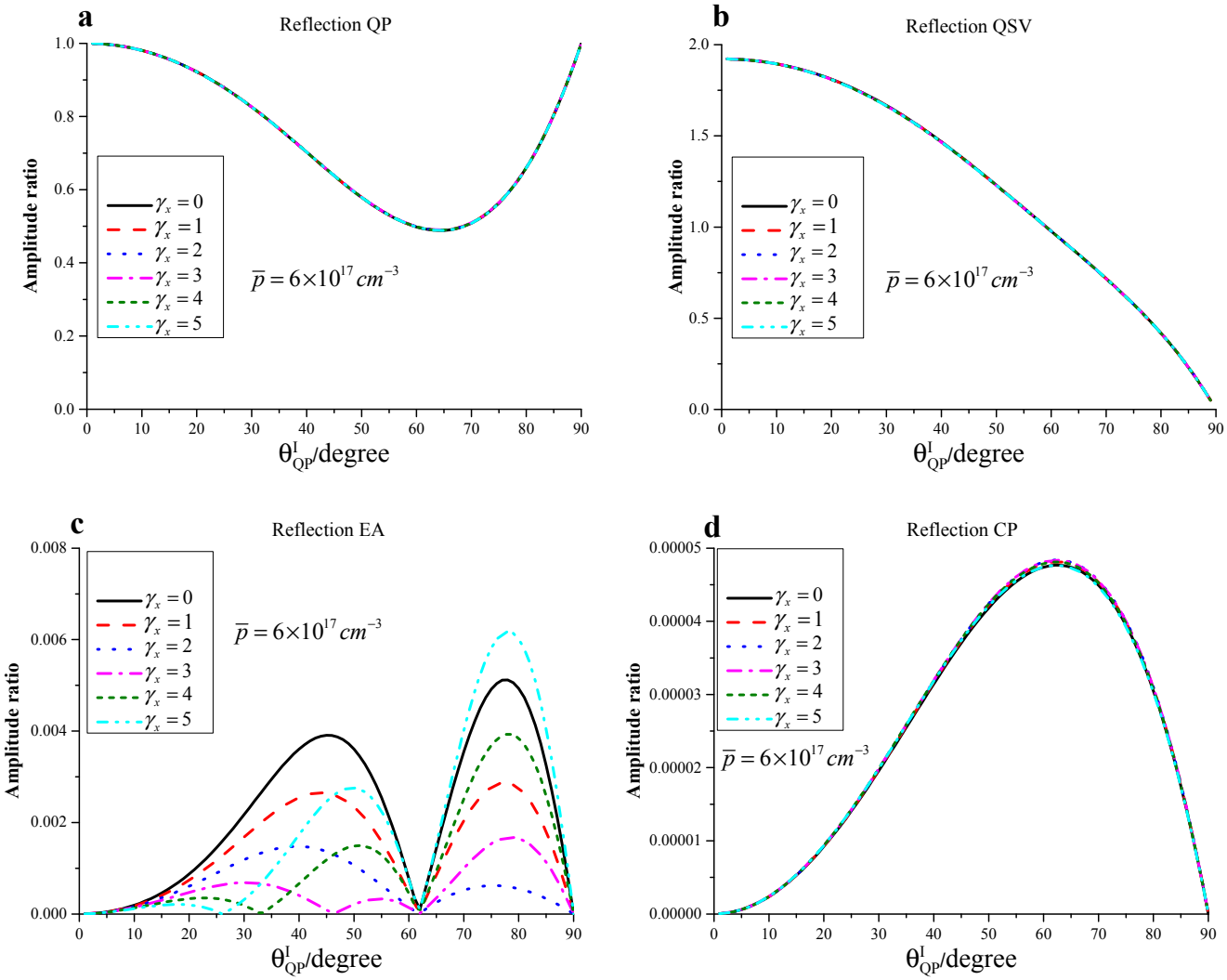

Fig. 9. The influences of the biasing electric field on the reflection amplitude ratios in the case of incident QP wave.($\gamma_z = 0$, $\omega = 10^{10}$ rad/s)

physic fields coupled waves, the interaction energy fluxes among various reflection waves and the incident wave are not zeros. Fig. 12 shows the energy flux balance check for the two cases, i.e. without consideration of the interaction energy flux and with consideration of the interaction energy flux. It is found that the energy flux balance is satisfied approximately without consideration of the interaction energy flux with the maximum error by 0.6 percent. When the interaction energy fluxes are taken into consideration, the energy flux balance can be better satisfied. This implies that the interaction energy fluxes are not the dominated energy flux, but they exist indeed in the piezoelectric

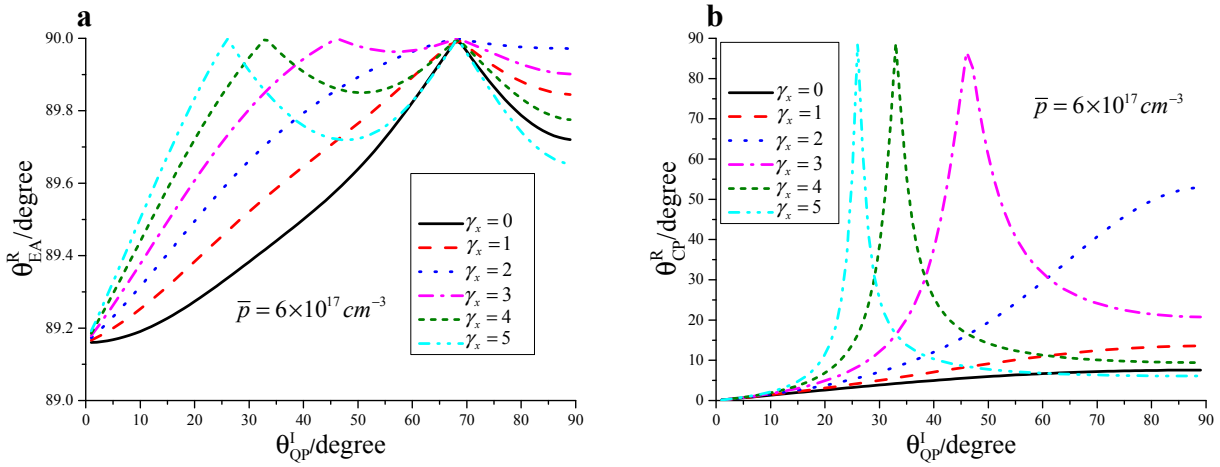

Fig. 10. The influences of the biasing electric field on the reflection angles in the case of incident QP wave ($\gamma_z = 0$, $\omega = 10^{10}$ rad/s).

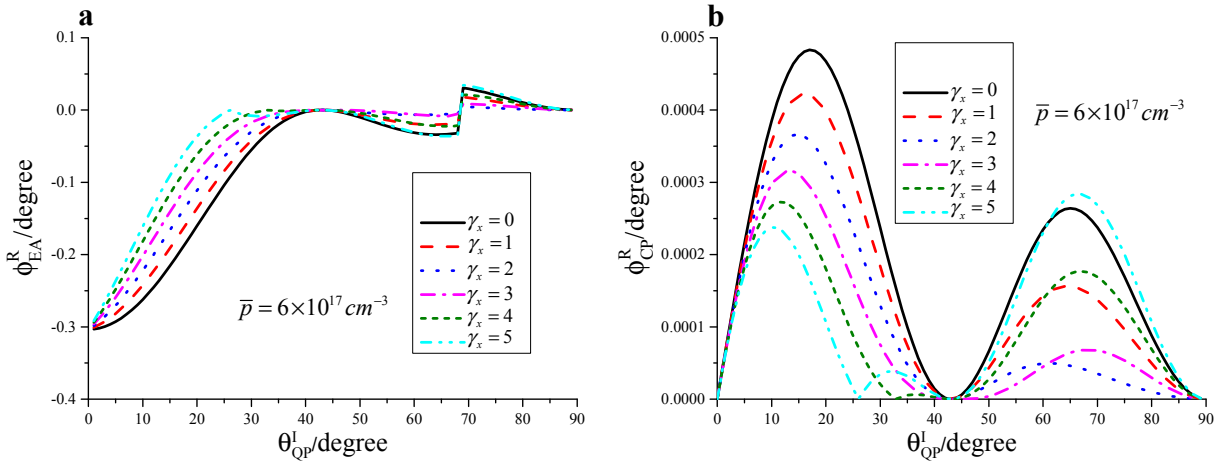

Fig. 11. The influences of the biasing electric field on the attenuation angles of the reflection waves in the case of incident QP wave ($\gamma_z = 0$, $\omega = 10^{10}$ rad/s).

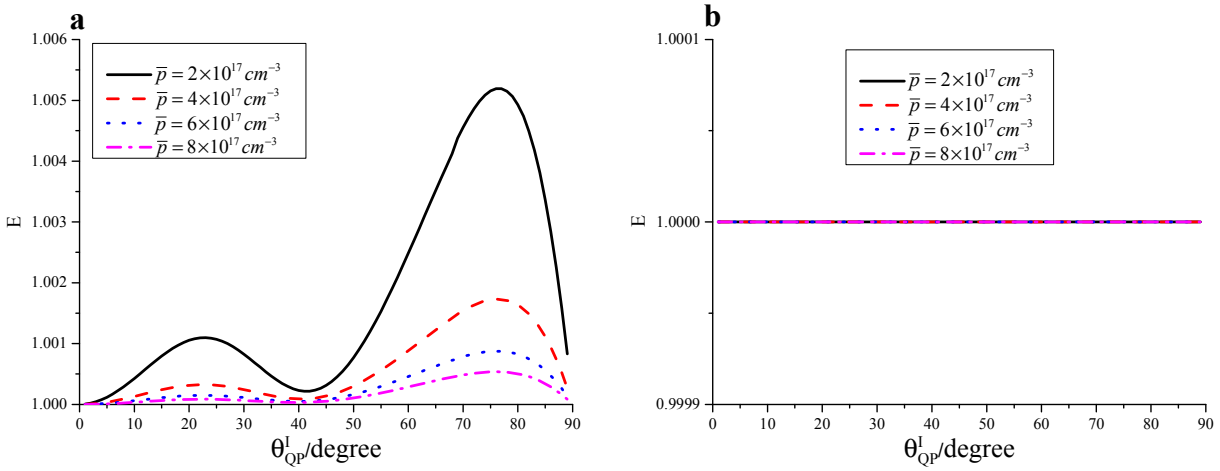

Fig. 12. Check on the energy flux balance in the case of incident QP wave. (a) without consideration of the interaction energy flux; (b) with consideration of the interaction energy flux ($\gamma = 0$, $\omega = 10^{10}$ rad/s).

semiconductor medium, and can influence the energy partition of partial waves at the boundary.

6. Conclusion

In a piezoelectric semiconductor, a mechanical perturbation usually motivates the displacement field, the electric potential field and the carrier density field simultaneously. These physical fields are coupled together and result in the multi-physical fields coupled waves. The existence of the electric current makes the multi-physical fields coupled waves not only dispersive but also attenuated. In the present work, the dispersive equation and the attenuated equation are first formulated for

the multi-physical fields coupled waves in an infinite piezoelectric semiconductor. Then, the reflection problem from a boundary which is mechanically free, electrically insulation and the dielectrically open circuit are studied. Based on the numerical simulation, the following conclusions can be drawn.

(1) The multi-physical fields coupled waves are not only dispersive but also attenuated. More than that, the propagation direction and the attenuation direction are not coincident in general. In other word, the multi-physical fields coupled waves are usually the inhomogeneous waves.
(2) The dispersion and attenuation features of the coupled waves in an infinite or semi-infinite piezoelectric semiconductor solid are very similar with that in the standard linear viscoelastic solid. Especially, there is the frequency sensitive zone of the dispersion and attenuation and the dispersion and attenuation features disappear at relative higher and lower frequency for both kinds of solids. Therefore, there is a phenomenological analogy between the piezoelectric semiconductor solid and the standard linear viscoelastic solid, although the root causes resulting in the dispersion and attenuation are different completely.
(3) The steady carrier density and the biasing electric field have the evident influence on the reflection EA wave and CP wave while only slight influence on the reflection QP wave and QSV wave. These influences include not only the reflection amplitudes, but also the reflection angles and attenuation angles of the reflection waves. Usually, the deviation between the propagation direction and the attenuation direction increases as the steady carrier density increases.
(4) The biasing electric field along the propagation direction can increase or decrease the amplitudes of waves which depend on the direction and magnitude of the biasing electric field. The amplitudes of waves may be amplified when the biasing electric field is sufficiently large.
(5) EA wave in the classical piezoelectric half-space (without the electric current) is always the surface wave, but it becomes the bulk wave in the piezoelectric semiconductor half-space apart from at a few of special incident angles, in general.
(6) Due to the attenuation nature of the multi-physical fields coupled waves, the interaction energy fluxes among the various reflection waves and the incident wave do not vanish. Therefore, the energy flux balance should include the interaction energy fluxes.

Acknowledgments

The work is supported by the Fundamental Research Funds for the Central Universities (FRF-TW-2018-005) and National Natural Science Foundation of China (No. 10972029).

Appendix A

$K_{11} = c_{11}k_x^2 + c_{44}k_z^2 - \rho\omega^2$, $K_{12} = K_{21} = (c_{13} + c_{44})k_x k_z$, $K_{33} = -\varepsilon_{11}k_x^2 - \varepsilon_{33}k_z^2$, $K_{13} = K_{31} = (e_{15} + e_{31})k_x k_z$, $K_{22} = c_{44}k_x^2 + c_{33}k_z^2 - \rho\omega^2$, $K_{23} = K_{32} = e_{15}k_x^2 + e_{33}k_z^2$, $K_{34} = q$, $K_{43} = \bar{p}\,(\mu_{11}k_x^2 + \mu_{33}k_z^2)$, $K_{44} = d_{11}k_x^2 + d_{33}k_z^2 + i(\mu_{11}\overline{E}_x k_x + \mu_{33}\overline{E}_z k_z - \omega)$.

Appendix B

$F_{1q} = c_{44}\,(k_{zq} + G_q k_x) + e_{15}H_q k_x$, $F_{2q} = c_{13}k_x + c_{33}k_{zq}G_q + e_{33}k_{zq}H_q$, $F_{3q} = c_{11}k_x + c_{13}G_q k_{zq} + e_{31}H_q k_{zq}$, $F_{4q} = e_{31}k_x + e_{33}G_q k_{zq} - \varepsilon_{33}H_q k_{zq}$, $F_{5q} = e_{15}(k_{zq} + G_q k_x) - \varepsilon_{11}H_q k_x$, $F_{6q} = -iq\,(\bar{p}\mu_{33}H_q + d_{33}Q_q)k_{zq} + q\mu_{33}\overline{E}_z Q_q$, $F_{7q} = -iqk_x(\bar{p}\mu_{11}H_q + d_{11}Q_q) + q\mu_{11}\overline{E}_x Q_q$.

Appendix C

$$Q_{QP(QSV)^I} = \frac{1}{2}\mathrm{Re}(F_{1q}\omega + F_{2q}G_q^*\omega + F_{4q}^*H_q\omega + F_{6q}^*H_q)U_{1q}U_{1q}^*\exp[-2\,\mathrm{Im}(k_x)x]$$

$$Q_{QP^R} = \frac{1}{2}\mathrm{Re}(F_{11}\omega + F_{21}G_1^*\omega + F_{41}^*H_1\omega + F_{61}^*H_1)L_1L_1^*U_{1q}U_{1q}^*\exp[-2\,\mathrm{Im}(k_x)x]$$

$$Q_{QSV^R} = \frac{1}{2}\mathrm{Re}(F_{13}\omega + F_{23}G_3^*\omega + F_{43}^*H_3\omega + F_{63}^*H_3)L_2L_2^*U_{1q}U_{1q}^*\exp[-2\,\mathrm{Im}(k_x)x]$$

$$Q_{EA^R} = \frac{1}{2}\mathrm{Re}(F_{15}\omega + F_{25}G_5^*\omega + F_{45}^*H_5\omega + F_{65}^*H_5)L_3L_3^*U_{1q}U_{1q}^*\exp[-2\,\mathrm{Im}(k_x)x]$$

$$Q_{CP^R} = \frac{1}{2}\mathrm{Re}(F_{17}\omega + F_{27}G_7^*\omega + F_{47}^*H_7\omega + F_{67}^*H_7)L_4L_4^*U_{1q}U_{1q}^*\exp[-2\,\mathrm{Im}(k_x)x]$$

$$Q_{QP(QSV)^IQP^R} = \frac{1}{2}\mathrm{Re}[(F_{1q}\omega + F_{2q}G_1^*\omega + F_{41}^*H_q\omega + F_{61}^*H_q)L_1^* + (F_{11}\omega + F_{21}G_q^*\omega + F_{4q}^*H_1\omega + F_{6q}^*H_1)L_1]U_{1q}U_{1q}^*\exp[-2\,\mathrm{Im}(k_x)x]$$

$$Q_{QP(QSV)^IQSV^R} = \frac{1}{2}\mathrm{Re}[(F_{1q}\omega + F_{2q}G_3^*\omega + F_{43}^*H_q\omega + F_{63}^*H_q)L_2^* + (F_{13}\omega + F_{23}G_q^*\omega + F_{4q}^*H_3\omega + F_{6q}^*H_3)L_2]U_{1q}U_{1q}^*\exp[-2\,\mathrm{Im}(k_x)x]$$

$$Q_{QP(QSV)^IEA^R} = \frac{1}{2}\mathrm{Re}[(F_{1q}\omega + F_{2q}G_5^*\omega + F_{45}^*H_q\omega + F_{65}^*H_q)L_3^* + (F_{15}\omega + F_{25}G_q^*\omega + F_{4q}^*H_5\omega + F_{6q}^*H_5)L_3]U_{1q}U_{1q}^*\exp[-2\,\mathrm{Im}(k_x)x]$$

$$Q_{QP(QSV)^ICP^R} = \frac{1}{2}\mathrm{Re}[(F_{1q}\omega + F_{2q}G_7^*\omega + F_{47}^*H_q\omega + F_{67}^*H_q)L_4^* + (F_{17}\omega + F_{27}G_q^*\omega + F_{4q}^*H_7\omega + F_{6q}^*H_7)L_4]U_{1q}U_{1q}^*\exp[-2\,\mathrm{Im}(k_x)x]$$

$$Q_{QP^RQSV^R} = \frac{1}{2}\mathrm{Re}[(F_{13}\omega + F_{23}G_1^*\omega + F_{41}^*H_3\omega + F_{61}^*H_3)L_1^*L_2 + (F_{11}\omega + F_{21}G_3^*\omega + F_{43}^*H_1\omega + F_{63}^*H_1)L_1L_2^*]U_{1q}U_{1q}^*\exp[-2\,\mathrm{Im}(k_x)x]$$

$$Q_{QP^REA^R} = \frac{1}{2}\mathrm{Re}[(F_{15}\omega + F_{25}G_1^*\omega + F_{41}^*H_5\omega + F_{61}^*H_5)L_1^*L_3 + (F_{11}\omega + F_{21}G_5^*\omega + F_{45}^*H_1\omega + F_{65}^*H_1)L_1L_3^*]U_{1q}U_{1q}^*\exp[-2\,\mathrm{Im}(k_x)x]$$

$$Q_{QP^RCP^R} = \frac{1}{2}\mathrm{Re}[(F_{17}\omega + F_{27}G_1^*\omega + F_{41}^*H_7\omega + F_{61}^*H_7)L_1^*L_4 + (F_{11}\omega + F_{21}G_7^*\omega + F_{47}^*H_1\omega + F_{67}^*H_1)L_1L_4^*]U_{1q}U_{1q}^*\exp[-2\,\mathrm{Im}(k_x)x]$$

$$Q_{QSV^REA^R} = \frac{1}{2}\mathrm{Re}[(F_{15}\omega + F_{25}G_3^*\omega + F_{43}^*H_5\omega + F_{63}^*H_5)L_2^*L_3 + (F_{13}\omega + F_{23}G_5^*\omega + F_{45}^*H_3\omega + F_{65}^*H_3)L_2L_3^*]U_{1q}U_{1q}^*\exp[-2\,\mathrm{Im}(k_x)x]$$

$$Q_{QSV^RCP^R} = \frac{1}{2}\mathrm{Re}[(F_{17}\omega + F_{27}G_3^*\omega + F_{43}^*H_7\omega + F_{63}^*H_7)L_2^*L_4 + (F_{13}\omega + F_{23}G_7^*\omega + F_{47}^*H_3\omega + F_{67}^*H_3)L_2L_4^*]U_{1q}U_{1q}^*\exp[-2\,\mathrm{Im}(k_x)x]$$

$$Q_{EA^RCP^R} = \frac{1}{2}\mathrm{Re}[(F_{17}\omega + F_{27}G_5^*\omega + F_{45}^*H_7\omega + F_{65}^*H_7)L_3^*L_4 + (F_{15}\omega + F_{25}G_7^*\omega + F_{47}^*H_5\omega + F_{67}^*H_5)L_3L_4^*]U_{1q}U_{1q}^*\exp[-2\,\mathrm{Im}(k_x)x]$$

where $q = 2$ indicates the incident QP wave, $q = 4$ indicates the incident QSV wave.

References

[1] B.A. Auld, Acoustic Fields and Waves in Solids, Wiley, New York, 1973.
[2] A.R. Hutson, D.L. White, Elastic wave propagation in piezoelectric semiconductors, J. Appl. Phys. 33 (1) (1962) 40–47.
[3] G. Weinreich, T.M. Sanders Jr, H.G. White, Acoustoelectric effect in n-type germanium, Phys. Rev. 114 (1) (1959) 33.
[4] D.R. Dietz, L.J. Busse, M.J. Fife, Acoustoelectric detection of ultrasound power with composite piezoelectric and semiconductor devices, IEEE Trans. Ultrason. Ferroelectr. Freq. Control 35 (2) (1988) 146–151.
[5] J.N. Sharma, K.K. Sharma, A. Kumar, Surface waves in a piezoelectric–semiconductor composite structure, Int. J. Solids Struct. 47 (6) (2010) 816–826.
[6] J.N. Sharma, K.K. Sharma, A. Kumar, Acousto-diffusive waves in a piezoelectric-semiconductor-piezoelectric sandwich structure, World J. Mech. 1 (5) (2011) 247–255.
[7] J.N. Sharma, K.K. Sharma, A. Kumar, Modelling of acoustodiffusive surface waves in piezoelectric-semiconductor composite structures, J. Mech. Mater. Struct. 6 (6) (2011) 791–812.
[8] D.L. White, Amplification of ultrasonic waves in piezoelectric semiconductors, J. Appl. Phys. 33 (8) (1962) 2547–2554.
[9] J.S. Yang, H.G. Zhou, Wave propagation in a piezoelectric ceramic plate sandwiched between two semiconductor layers, Int. J. Appl. Electromagn. Mech. 22 (1, 2) (2005) 97–109.
[10] C. Gu, F. Jin, Shear-horizontal surface waves in a half-space of piezoelectric semiconductors, Philos. Mag. Lett. 95 (2) (2015) 92–100.
[11] G.S. Kino, Acoustoelectric interactions in acoustic-surface-wave devices, Proc. IEEE 64 (5) (1976) 724–748.
[12] P. Hiralal, H.E. Unalan, G.A.J. Amaratunga, Nanowires for energy generation, Nanotechnology 23 (19) (2012) 194002.
[13] B. Kumar, S.W. Kim, Energy harvesting based on semiconducting piezoelectric ZnO nanostructures, Nano Energy 1 (3) (2012) 342–355.
[14] P. Li, F. Jin, J. Yang, Effects of semiconduction on electromechanical energy conversion in piezoelectrics, Smart Mater. Struct. 24 (2) (2015) 025021.
[15] C. Zhang, X. Wang, W. Chen, et al., Carrier distribution and electromechanical fields in a free piezoelectric semiconductor rod, J. Zhejiang Univ. Sci. A 17 (1) (2016) 37–44.
[16] C.L. Zhang, X.Y. Wang, W.Q. Chen, et al., Propagation of extensional waves in a piezoelectric semiconductor rod, AIP Adv. 6 (4) (2016) 045301.
[17] J.N. Sharma, A. Sharma, Reflection of acoustodiffusive waves from the boundary of a semiconductor halfspace, J. Appl. Phys. 108 (3) (2010) 033712.
[18] J.N. Sharma, A. Sharma, Reflection and transmission of acoustic waves at semiconductor-liquid interface, AIP Adv. 1 (3) (2011) 032137.
[19] E.S. Krebes, The viscoelastic reflection/transmission problem: two special cases, Bull. Seismol. Soc. Am. 73 (6A) (1983) 1673–1683.
[20] Y. Pang, Y.S. Wang, J.X. Liu, et al., Reflection and refraction of plane waves at the interface between piezoelectric and piezomagnetic media, Int. J. Eng. Sci. 46 (11) (2008) 1098–1110.
[21] X. Guo, P. Wei, L. Li, et al., Influences of mechanically and dielectrically imperfect interfaces on the reflection and transmission waves between two piezoelectric half spaces, Int. J. Solids Struct. 63 (2015) 184–205.
[22] F. Jiao, P. Wei, L. Li, Wave propagation through an inhomogeneous slab sandwiched by the piezoelectric and the piezomagnetic half spaces, Ultrasonics 73 (2017) 22–33.
[23] F. Jiao, P. Wei, Y. Li, Wave propagation through a flexoelectric piezoelectric slab sandwiched by two piezoelectric half-spaces, Ultrasonics 82 (2018) 217–232.
[24] T.M. Barnes, K. Olson, C.A. Wolden, On the formation and stability of p-type conductivity in nitrogen-doped zinc oxide, Appl. Phys. Lett. 86 (11) (2005) 112112.
[25] J.C. Fan, K.M. Sreekanth, Z. Xie, et al., p-Type ZnO materials: theory, growth, properties and devices, Prog. Mater. Sci. 58 (6) (2013) 874–985.
[26] J. Sladek, V. Sladek, E. Pan, et al., Fracture analysis in piezoelectric semiconductors under a thermal load, Eng. Fract. Mech. 126 (2014) 27–39.
[27] P.J. Wei, S.Y. Zhang, Singularity of dynamic stress fields around an interface crack between viscoelastic bodies, Int. J. Fract. 126 (2) (2004) 165–177.
[28] Y.P. Zhao, P.J. Wei, The band gap of 1D viscoelastic phononic crystal, Comput. Mater. Sci. 46 (3) (2009) 603–606.
[29] P.J. Wei, Y.P. Zhao, The influence of viscosity on band gaps of 2D phononic crystal, Mech. Adv. Mater. Struct. 17 (6) (2010) 383–392.